White Rose Research Online

eprints@whiterose.ac.uk
https://eprints.whiterose.ac.uk
Universities of Leeds, Sheffield and York

Deposited via The University of Sheffield.

White Rose Research Online URL for this paper:
https://eprints.whiterose.ac.uk/id/eprint/174874/

Version: Published Version

---

**Proceedings Paper:**
Tipuric, M., Wagg, D. and Sims, N. (2019) Magnetorheological bypass valve design for a semi-active inerter. In: Erturk, A., (ed.) Active and Passive Smart Structures and Integrated Systems XIII. SPIE Smart Structures + Nondestructive Evaluation, 03-07 Mar 2019, Denver, Colorado, United States. Proceedings of SPIE (10967). Society of Photo Optical Instrumentation Engineers (SPIE). Article no: UNSP 109671L. ISBN: 9781510625891. ISSN: 0277-786X. EISSN: 1996-756X.

https://doi.org/10.1117/12.2514278

---

Copyright 2019 Society of Photo Optical Instrumentation Engineers (SPIE). One print or electronic copy may be made for personal use only. Systematic reproduction and distribution, duplication of any material in this publication for a fee or for commercial purposes, or modification of the contents of the publication are prohibited.

**Reuse**
Items deposited in White Rose Research Online are protected by copyright, with all rights reserved unless indicated otherwise. They may be downloaded and/or printed for private study, or other acts as permitted by national copyright laws. The publisher or other rights holders may allow further reproduction and re-use of the full text version. This is indicated by the licence information on the White Rose Research Online record for the item.

**Takedown**
If you consider content in White Rose Research Online to be in breach of UK law, please notify us by emailing eprints@whiterose.ac.uk including the URL of the record and the reason for the withdrawal request.

PROCEEDINGS OF SPIE

SPIEDigitalLibrary.org/conference-proceedings-of-spie

# Magnetorheological bypass valve design for a semi-active inerter

Matthew Tipuric, David Wagg, Neil Sims

Matthew Tipuric, David Wagg, Neil Sims, "Magnetorheological bypass valve design for a semi-active inerter ," Proc. SPIE 10967, Active and Passive Smart Structures and Integrated Systems XII, 109671L (21 March 2019); doi: 10.1117/12.2514278

SPIE.

Event: SPIE Smart Structures + Nondestructive Evaluation, 2019, Denver, Colorado, United States

Downloaded From: https://www.spiedigitallibrary.org/conference-proceedings-of-spie on 25 Jul 2019 Terms of Use: https://www.spiedigitallibrary.org/terms-of-use

# Magnetorheological bypass valve design for a semi-active inerter

Matthew Tipuric[a,b], David Wagg[b], and Neil Sims[b]

[a]Industrial Doctorate Centre in Machining Science, Advanced Manufacturing Research Centre with Boeing, University of Sheffield, Rotherham, S60 5TZ, UK
[b]Department of Mechanical Engineering, Sir Frederick Mappin Building, Mappin Street, Sheffield, S1 3JD, UK

## ABSTRACT

Inerters are a class of vibration absorber which create a resistive force proportional to the relative acceleration across their two terminals. It has been previously shown that it is possible to create an inerter where the size of this force is variable, through use of a bypass channel controlled by a magnetorheological (MR) valve. However, the requirements and restrictions of such a device mean that existing design methodologies are insufficient. For example, as the pressure drop in the rest of the device is dependent on both the geometry of the device and the velocity of the fluid, it is important to design the valve with this in mind, in order to maximise the control range of the entire device, rather than just the valve itself. This work considers the effects of varying the dimensions of a valve and presents a performance metric to be used to allow comparison of different designs. The results are demonstrated as part of a model of a fluid inerter system.

**Keywords:** Magnetorheological fluid; inerter; semi-active damper; valve

## 1. INTRODUCTION

The inerter is a device which creates a force (known as the inertance) proportional to the relative acceleration of its terminals[1] and, as such, have uses in the field of vibration control, including as parts of vehicle suspension systems or for protecting buildings from earthquakes and bridges from wind. Previous work by the authors has investigated the potential of semi-active inerter designs, using magnetorheological (MR) fluid within a hydraulic circuit to allow the inertance to be controlled using a valve.[2] Such a design would greatly increase the utility of the inerter, allowing it to operate more efficiently under a wider range of dynamic vibrations, as well as making a whole range of semi-active control strategies possible.

The proposed design entails using an MR valve within a bypass channel, controlling the flow rate through the helical channel of a fluid inerter. This type of valve is well understood within the context of magnetorheological damping, with optimisation schema already existing for the case when the valve function is to provide a resistive force within a piston. However, the use here is different, both in aim and in the constraints imposed. In order for an appropriate design to be possible, it is vital to have some metric by which different valves can be compared.

In Section 2, the mechanism of the semi-active bypass inerter will be discussed, including the model of the MR valve. In Section 3 a f performance metric for the valve is derived, with the design implications of these being detailed in Section 4. Finally, the paper will be concluded in Section 5.

Further author information: (Send correspondence to Matthew Tipuric)
M. Tipuric: E-mail: mrtipuric1@sheffield.ac.uk

Active and Passive Smart Structures and Integrated Systems XII, edited by Alper Erturk, Proc. of SPIE
Vol. 10967, 109671L · © 2019 SPIE · CCC code: 0277-786X/19/$18 · doi: 10.1117/12.2514278



Downloaded From: https://www.spiedigitallibrary.org/conference-proceedings-of-spie on 25 Jul 2019
Terms of Use: https://www.spiedigitallibrary.org/terms-of-use

## 2. THEORY

The device being investigated in this paper is based on the helical inerter, which was modelled, for example, by Swift et al.[3] In a helical inerter the movement of a piston relative to the cylinder body causes the working fluid to flow through the helix. The rotation of the mass of the fluid creates an inertial effect, which is proportional to acceleration, while the pressure drop creates a force non-linearly proportional to the velocity. Thus the total resistive force of the device can be approximated as

$$F = b\ddot{x} + A_1\left(A\frac{A_1}{A_H}\dot{x} + B\left(\frac{A_1}{A_H}\dot{x}\right)^2\right), \tag{1}$$

where

$$\begin{aligned} b &= \frac{m_H}{1+\frac{H}{2\pi r_4}}\left(\frac{A_1}{A_H}\right)^2 \\ A &= 8.77\frac{\mu l}{r_3^2} \\ B &= 0.04845\frac{\rho l}{\sqrt{r_3 r_4}} \end{aligned} \tag{2}$$

Here, $A_1 = \pi(r_2^2 - r_1^2)$ and $A_H = \pi r_3^3$ are the areas of the cylinder and helix, respectively, as defined in Figure 1, $l$ is the length of the helix and $m_H = \rho l A_H$ is the mass of the fluid in the helix. $\mu$ and $\rho$ are the viscosity and density of the working fluid, respectively.

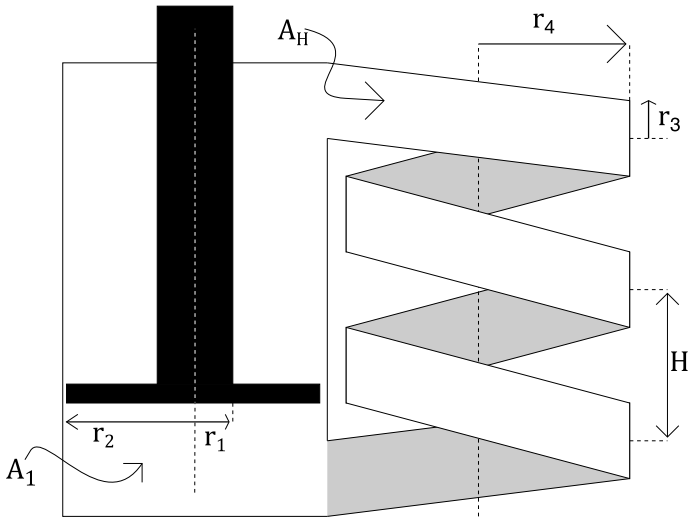


Figure 1: The main dimensions of a helical inerter.

By considering the conservation of energy in the ideal device, it can be seen that the linear kinetic energy from the movement of the piston is converted into rotational kinetic energy of the fluid in the helix

$$\frac{1}{2}b\dot{x}^2 = \frac{1}{2}J\dot{\theta}^2, \tag{3}$$

where $\dot{\theta}$ is the fluid's angular velocity[4] and $J = m_H r_4^2$ is its moment of inertia. By approximating this as the angular velocity of the fluid at the streamline $\dot{\theta} = \frac{u}{r_4}$, Equation 3 can be rewritten as

$$b = m_H\left(\frac{u}{\dot{x}}\right)^2, \tag{4}$$



Downloaded From: https://www.spiedigitallibrary.org/conference-proceedings-of-spie on 25 Jul 2019
Terms of Use: https://www.spiedigitallibrary.org/terms-of-use

which, for the standard fluid inerter is equivalent to the form in Equation 2, assuming that incompressible flow and that $\frac{H}{2\pi r_4} \ll 1$.

The bypass fluid inerter, shown in Figure 2, includes the addition of a bypass channel in parallel with the helix, which can be controlled with an MR valve, if MR fluid is used as the working fluid. Assuming incompressible, adiabatic flow, the total volumetric flow rate will in the cylinder will be the sum of those in the helix and the valve and there will be an equal pressure drop across both of these:

$$Q_1 = Q_H + Q_v \tag{5}$$

$$\Delta p_H = \Delta p_v, \tag{6}$$

where subscripts 1, $H$ and $v$ refer to the cylinder, helix and valve, respectively. To calculate the inertance, we require the fluid velocity in the helix, $u = \frac{Q_H}{A_H}$, and so we need to find the flow rate and pressure across the valve. It should also be noted that the pressure drop across the valve is composed of two main components, the pressure drop caused by the active section, $\Delta p_a$, where the fluid interacts with the magnetic field and that from by the passive section, $\Delta p_v$, which is purely Newtonian.

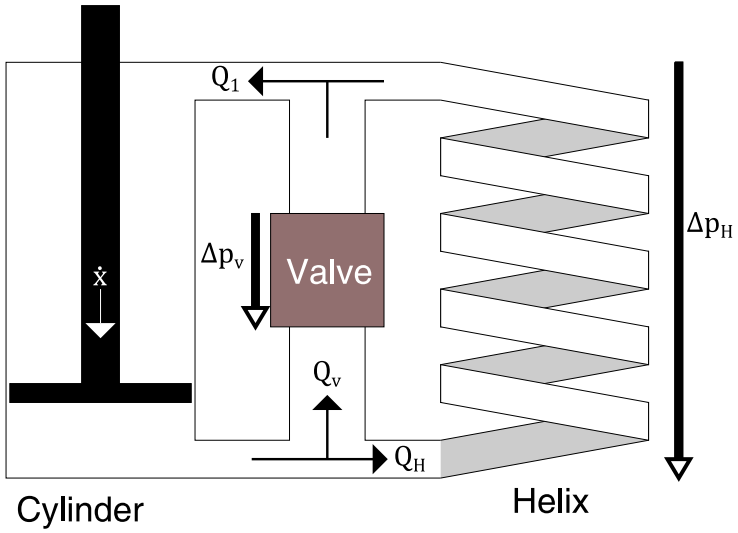


Figure 2: A schematic of the bypass inerter for which the valve is to be designed.

A conventional MR valve, as shown in Figure 3 has an annular flow channel, which is crossed by magnetic field lines at two areas, induced by an electric current in the wire. This magnetic field interacts with the magnetisable particles suspended in the MR fluid, causing them to cross link, increasing the fluid's resistance to flow. This behaviour can be well represented as that of a Bingham fluid, a class of non-Newtonian fluid characterised by having a shear stress of

$$\tau = \mu \frac{\mathrm{d}u}{\mathrm{d}y} + \tau_b \operatorname{sgn}\left(\frac{\mathrm{d}u}{\mathrm{d}y}\right). \tag{7}$$

For annular magnetorheological valves with a sufficiently large ratio of radius, $r_v$, to gap height, $h$, the flow can be further approximated as that between two flat plates with width $b = 2\pi r_v$. The two-dimensional flow profile is then as shown in Figure 3, with a central plug of non-dimensional width $\bar{\delta} = \frac{\delta}{h}$ where no shear exists.[5] The size of this plug can be found by balancing the force from the Bingham stress on the plug with the wall stress, $\tau_w = \frac{\Delta p_a h}{2 l_a}$:

$$\bar{\delta} = \frac{\tau_b}{\tau_w} = \frac{2 l_a \tau_b}{\Delta p_a h}. \tag{8}$$



Downloaded From: https://www.spiedigitallibrary.org/conference-proceedings-of-spie on 25 Jul 2019
Terms of Use: https://www.spiedigitallibrary.org/terms-of-use

As no shear occurs within the plug, for flow to occur in the helix the plug must be smaller than the channel width, $\bar{\delta} > 1$ so

$$\Delta p_a > \frac{2l_a\tau_b}{h}. \tag{9}$$

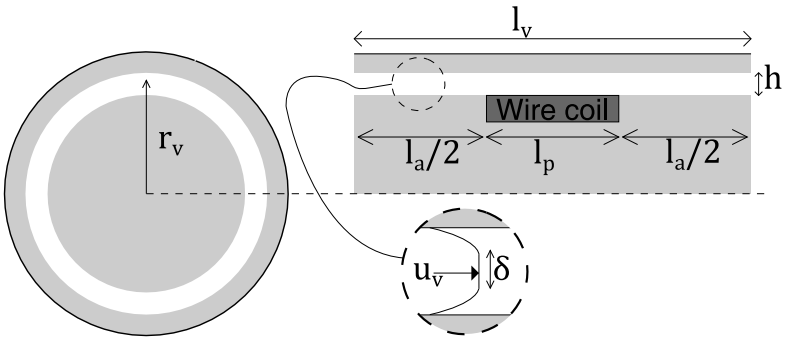


Figure 3: A magnetorheological valve, with an example of the assumed velocity profile shown.

From Equation 6, the pressure in the valve is equal to that in the helix. As the contribution from the passive length of the valve is purely proportional to the flow velocity within it, for the limiting case of $Q_v = 0$, $P_a = P_v = P_h$. This means that, for a given Bingham yield stress in the valve, the point at which flow commences can be found from the positive root of

$$B\Big(\frac{Q_1}{A_H}\Big)^2 + A\frac{Q_1}{A_H} - \frac{2l_a\tau_b}{h} = 0 \tag{10}$$

The root must be positive as the valve force is purely resistive to motion i.e. the flow in the valve and helix must always be in the same direction and so this critical value for the cylinder flow rate can be found to be

$$Q_1^* = \frac{A_H}{2B}\Big(\sqrt{A^2 + 8B\frac{l_a\tau_b}{h}} - A\Big) \tag{11}$$

This means that the behaviour of the bypass inerter can be divided into two parts. Firstly, if $Q_1 \leq Q_1^*$, $Q_H = Q_1$ and so the device works as a conventional inerter, represented by Equation 1. Secondly, if $Q_1 > Q_1^*$,

$$Q_H = Q_1 - \frac{bh^3}{6\mu l_a}(1-\bar{\delta})^2(1+0.5\bar{\delta})\frac{\Delta p_a}{2} \tag{12}$$

As the value of $\Delta p_a$ is itself dependent on $\Delta p_H$ and therefore $Q_H$, a general solution for Equation 12 is not trivial to find and, for the purposes of valve design, not particularly useful. We can instead consider another limiting solution, that of $\bar{\delta} = 0$, i.e. zero Bingham stress or no magnetic field. In this case, the flow in the helix can be found by

$$Q_H = \frac{6\mu l_v A_H^2}{bh^3 B}\Big(\sqrt{\big(1 + \frac{bh^3 A}{12\mu l_v A_H}\big)^2 + Q_1\frac{bh^3 B}{3\mu l_v A_H^2}}\Big) - \big(1 + \frac{bh^3 A}{12\mu l_v A_H}\big) \tag{13}$$

Thus the inertance provided by the device can generally be represented by a control range as shown in Figure 4, consisting of the velocity independent 'on state' inertance, the velocity dependent 'off-state' inertance and a Bingham stress dependent critical velocity $\dot{x}^* = \frac{Q_1^*}{A_1}$ after which the behaviour transitions non-linearly from one to the other. Table 1 lists which device parameters impact each of these values. It can be seen that the on-state inertance is not impacted by valve geometry and so is not of interest from a valve design perspective.



Downloaded From: https://www.spiedigitallibrary.org/conference-proceedings-of-spie on 25 Jul 2019
Terms of Use: https://www.spiedigitallibrary.org/terms-of-use

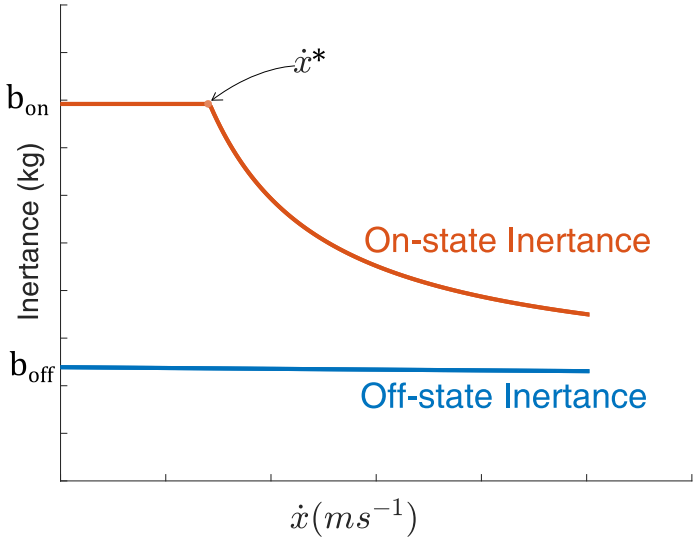

Figure 4: A schematic example control range of a bypass inerter.

| Parameter | Impacted by | | | |
|---|---|---|---|---|
| | Helix dimensions | Fluid Properties | Valve dimensions | Bingham Stress |
| On-state Inertance | ✓ | ✓ | - | - |
| Off-state Inertance | ✓ | ✓ | ✓ | - |
| Critical Velocity | ✓ | ✓ | ✓ | ✓ |

Table 1: Dependence of key values on different device parameters

## 3. DESCRIBING FUNCTION

MR valves are sometimes compared by their dynamic range:[6] the ratio of force at the highest achievable field strength to that in the off-state. However, in the case of the semi-active inerter, it is the inertance of the device as a whole that matters. As shown by the schematic diagram in Figure 4, this inertance range is velocity dependent.

As mentioned in Section 2, when in the on-state, the device acts as a traditional inerter and so the forms of the inertance equation in Equations 2 and 4 are equivalent, giving

$$b_{on} = m_H \left(\frac{A_1}{A_2}\right)^2. \tag{14}$$

To meaningfully compare this with the off-state, Equation 4 can be rewritten in terms of flow rates to reach

$$b_{off} = m_H \left(\frac{Q_H}{Q_1}\frac{A_1}{A_2}\right)^2 = \left(\frac{Q_H}{Q_1}\right)^2 b_{on}. \tag{15}$$

Thus, maximising the control range for any given piston velocity, $\frac{b_{on}}{b_{off}}$ means minimising the ratio $\left(\frac{Q_H}{Q_1}\right)^2$.

First, we need to find the pressure equations in terms of the flow rates. For the helix this is

$$\Delta p_H = A' Q_H + B' Q_H^2, \tag{16}$$

from Equation 1, where $A' = \frac{A}{A_H}$ and $B' = \frac{B}{A_H^2}$. The pressure drop across the valve is

$$\Delta p_v = C' Q_v, \tag{17}$$

where $C' = \frac{12\mu l_v}{bh^3}$ is the Newtonian valve pressure constant. By equating the pressure drop across the valve and the helix, we can find the mass flow rate in the helix with respect to that in the piston to be

$$Q_H = \frac{\sqrt{(A'+C')^2 + 4B'C'Q_1} - (A'+C')}{2B'}. \tag{18}$$



Downloaded From: https://www.spiedigitallibrary.org/conference-proceedings-of-spie on 25 Jul 2019
Terms of Use: https://www.spiedigitallibrary.org/terms-of-use

Table 2: Dimensions of the example device modelled.

| Variable | Value |
|---|---|
| $A_1$ | $1.26\text{x}10^{-2}\text{m}^2$ |
| $A_H$ | $1.27\text{x}10^{-4}\text{m}^2$ |
| $r_4$ | 0.09m |
| $l$ | 1.76m |
| $\rho$ | $3600\text{kgm}^{-3}$ |
| $\mu$ | 0.45Pas |

By dividing the square of this through by $Q_1^2$ and rearranging, the function to be minimised can be shown to be

$$f_1 = \frac{A' + C'}{2B'^2}\Big((A' + C') - \sqrt{(A' + C')^2 + 4B'C'Q_1}\Big)Q_1^{-2} + \frac{C'}{B'}Q_1^{-1}. \tag{19}$$

This function can be seen plotted as a function of $Q_1$ in Figure 5 for an example device, designed to provide 80kg of on-state inertance with 0.8 kg of fluid in the helix. The parameters of the device are detailed in Table 2 . Across a large range of flow rates, the non-linear behaviour of this function is obvious. However, in many cases such high flow rates are inappropriate. For the example device under consideration, a flow rate of $Q_1 = 1$ would equate to a piston velocity of $\dot{x} = 796\text{ms}^{-1}$, significantly higher than the expected operational maximum of $\dot{x} = 0.1\text{ms}^{-1}$, $Q_1 = 1.26\text{x}10^{-4}\text{m}^3\text{s}^{-1}$. For such a flow rate, the behaviour is more linear. For the current values, a least-squares approximation provides accuracy to within 1% up to a flow rate of $1.2\text{x}10^{-4}\text{m}^3\text{s}^{-1}$, as shown in Figure 6. In addition, for small flow ranges, the difference in maximum and minimum values may be so small as to be negligible, meaning that the inertance range can be considered to be independent of $Q_1$.

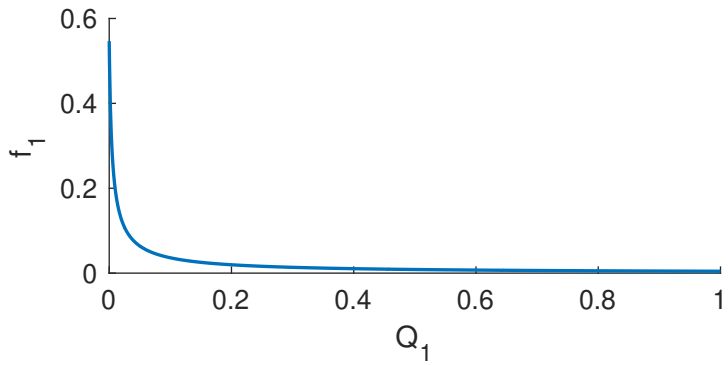

Figure 5: Function $f_1$.

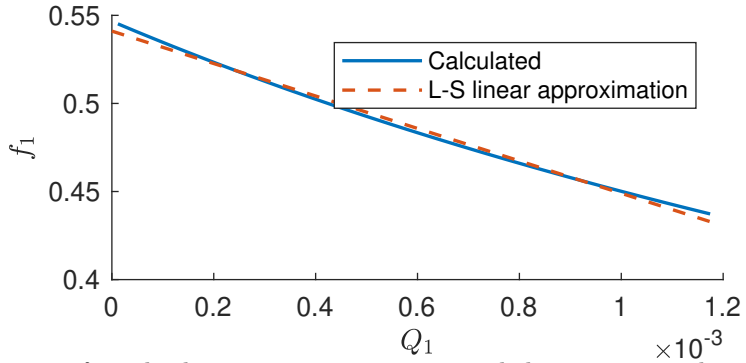

Figure 6: Function $f_1$ and a linear approximation, rescaled to a more realistic flow range.



Downloaded From: https://www.spiedigitallibrary.org/conference-proceedings-of-spie on 25 Jul 2019
Terms of Use: https://www.spiedigitallibrary.org/terms-of-use

## 4. VALVE DESIGN

As $f_1$ is to be minimised, it follows that a lower value for $C'$ is desirable. As

$$C' = \frac{12\mu l_v}{bh^3}, \tag{20}$$

this can be achieved either by increasing the valve circumference, $b = 2\pi r_v$, or gap height, $h$, or by reducing the valve length, $l_v$. This makes physical sense, as either shortening the valve or increasing its cross sectional area will have the effect of reducing the Newtonian pressure drop across it for a given flow rate.

It is not possible to reduce $C'$ arbitrarily to zero, as various constraints exist on the possible dimensions of the valve. The first of these is the maximum critical flow rate, i.e. the critical flow rate when the magnetic field is providing the largest achievable resistance to flow. For the inerter to be effective across its entire velocity range, it is necessary that this is higher than the maximum operational flow rate, which is controlled by the maximum expected piston velocity. By rearranging Equation 11, it can be seen that this sets a maximum ratio of the gap height to the active length of the valve as

$$D_0 = \frac{h}{l_a} \leq \frac{8B'\tau_b^{max}}{(Q_1^{max} + A')^2 - A'^2}. \tag{21}$$

In Ref.[7] a valve optimisation method is proposed for valves constrained in their radius, length and gap height. It is based on setting the areas through which the magnetic flux flows to be equal, thus avoiding bottlenecks being created by premature saturation in one area. Using the notation in Figure 7, these areas are the valve core, annular flux return and the flanges, $A_c = \pi t_a^2$, $A_{fr} = \pi(r_v^2 - (t_a + h + wc)^2)$ and $A_f = 2\pi t_a t_b$. In this case, the same criterion can be used, however the valve dimensions are not constrained in the same way. Instead, the constraints to be used are the valve radius, as this is judged to be the most likely parameter to be fixed by the design as a whole, and Equation 21.

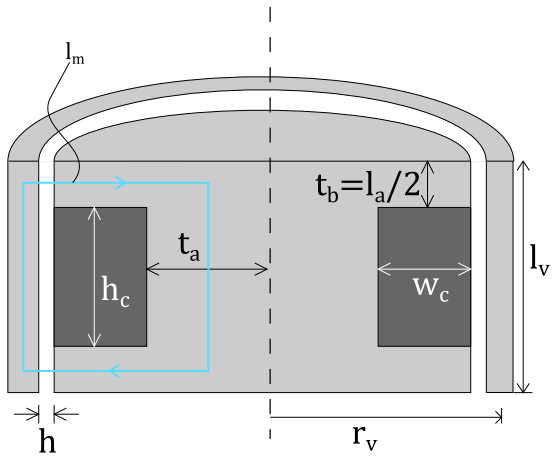

Figure 7: Dimensions used in equalising the valve areas.

By setting $A_c = A_f$, it can be shown that the active length must be equal to the radius of the core of the valve, $l_a = t_a$. As Equation 21 is dependant on the cube of $h$, increasing the gap height is more impactful on performance than decreasing the valve length. This means minimising the ratio in Equation 21, setting $h = D_0 l_a$. By substituting this value into the definition of flux return area and setting it equal to the valve core, $A_{fr} = A_c$, we find that the core radius, $t_a$, must be the positive root of

$$(1 + D^2)t_a^2 + 2Dw_c t_a + (w_c^2 - r_v^2) = 0, \tag{22}$$

where $D = 1 + \frac{D_0}{2} = 1 + \frac{h}{t_a}$. This allows $t_a$ and $h$ to be set as a function of coil width, $w_c$.



Downloaded From: https://www.spiedigitallibrary.org/conference-proceedings-of-spie on 25 Jul 2019
Terms of Use: https://www.spiedigitallibrary.org/terms-of-use

By considering the complete path of the magnetic field induced by the coil, we find that

$$NI^{max} = H_m l_m + 2H_f h, \tag{23}$$

where $N$ is the number of wire turns, $I^{max}$ is the maximum allowable current in the wire, $H_m$ and $H_f$ are the magnetic field in the valve material and MR fluid, respectively, and $l_m \approx r_v + w_c - h + 2(h_c + t_b)$ is the average path length of magnetic field in the valve metal,[8] as shown in Figure 7. $H_f$ can be found from the permeability curve of the MR fluid used, using the value which maximises $\tau_b$. $H_m$ can be found from the valve metal's permeability curve, using the value at $B_m = \frac{2\pi t_b(t_a+t_b+\frac{h}{2})}{\pi t_a^2} B_f$ (from the ratio of the area of the fluid to the core). If the number of turns can be approximated as $N \approx \frac{w_c h_c}{d_w^2}$, where $d_w$ is the diameter of the wire used, then from Equation 23,

$$h_c = \frac{H_m(r_v + w_c + 2t_b - h) + 2H_f h}{I^{max}\frac{w_c}{d_w^2} - 2H_m} \tag{24}$$

If the wire diameter is set, then both Equations 21 and 24 are dependent on $w_c$ only. From Equation 20, we need to find the value of $w_c$ which minimises $\frac{l_v}{h^3} = \frac{h_c + \frac{t_a}{2}}{D_0 t_a}$.

### Optimisation scheme

At this point, the valve parameters are set. For clarity, these steps are repeated below:

1. Maximise $r_v$ within design constraints.
2. Find $t_a$ (and hence $l_a$) with respect to $w_c$ using from the positive root of Equation 22. Use Equation 21 to find $h$ with respect to $w_c$.
3. Use equation 24 to find $h_c$, and hence $l_v = t_a + h_c$ with respect to $w_c$ .
4. Use these values to minimise $\frac{l_v}{h^3}$, which in turn minimises Equation 20.

## 4.1 Example Calculations

The optimisation scheme was used to design two valves for the inerter detailed in table 1, with a maximum piston velocity of $0.1\text{ms}^{-1}$. One valve was limited to a radius of 32mm, the other to 64mm. The recommended values for these two cases are listed in Table 3 and the inertance range for each is shown in Figure 8. It can be seen that the recommended gap height is significantly larger than in the type of valve used in dampers, this is due to the lower forces required in this context. The significant increase in performance from doubling the valve radius should also be noticed.

Table 3: Key dimensions of the optimised valve designs.

| $r_v$ (mm) | $t_a$ (mm) | $w_c$ (mm) | $h$ (mm) | $l_v$ (mm) |
|---|---|---|---|---|
| 32.0 | 19.0 | 5.8 | 1.0 | 31.4 |
| 64.0 | 39.0 | 9.7 | 2.0 | 53.8 |



Downloaded From: https://www.spiedigitallibrary.org/conference-proceedings-of-spie on 25 Jul 2019
Terms of Use: https://www.spiedigitallibrary.org/terms-of-use

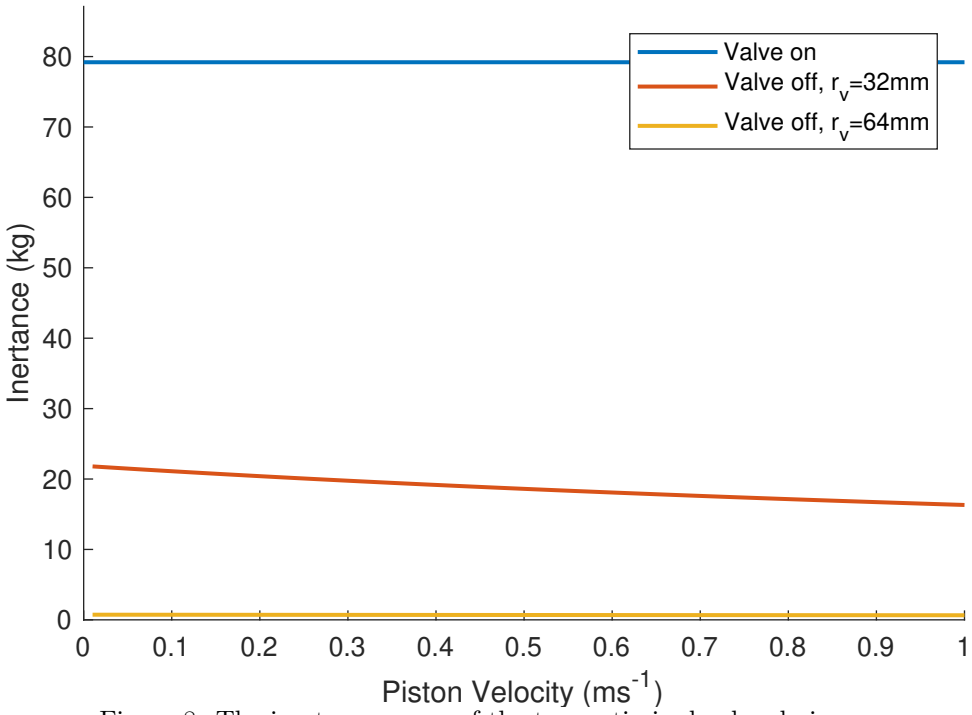

Figure 8: The inertance range of the two optimised valve designs.

## 5. CONCLUSION

When designing a magnetorheological valve to be used within a semi-active inerter, it is no longer sufficient to only consider the dynamic range of the valve in isolation. This paper has presented a function to be minimised based on the control range of the inerter as a whole. This function can be used as a performance metric to compare the effects of changing key dimensions of the valve. An optimisation method was then proposed, and used to find valve designs for an example device. The performance improvements offered by increasing the valve radius were demonstrated

The optimisation scheme produced designs with larger gap heights than those in traditional designs. The physical limits of this due to the magnetic field strength required in the magnetorheological fluid, and the effects on power requirements remain to be explored. Verification of this design method is expected to form the basis of further work.


## Acknowledgments

This research was supported by EPSRC (grant EP/L016257/1). The authors gratefully acknowledge this support.


## REFERENCES


[1] M. C. Smith, "Synthesis of mechanical networks: the inerter," *Automatic Control, IEEE Transactions on* **47**(10), pp. 1648–1662, 2002.

[2] M. Tipuric, D. Wagg, and N. Sims, "Vibration suppression using the concept of a semi-active magnetorheological inerter device," *proceedings of the International Confernce on Uncertainty in Structural Mechanics 2018* , 2018.

[3] S. Swift, M. Smith, A. Glover, C. Papageorgiou, B. Gartner, and N. Houghton, "Design and modelling of a fluid inerter," *International Journal of Control* **86**(11), pp. 2035–2051, 2013.

[4] B. J. Gartner and M. C. Smith, "Damping and inertial hydraulic device," (US20130037362 A1), patent filed 2011.





Downloaded From: https://www.spiedigitallibrary.org/conference-proceedings-of-spie on 25 Jul 2019
Terms of Use: https://www.spiedigitallibrary.org/terms-of-use

[5] D. J. Peel and W. A. Bullough, "Prediction of electro-rheological valve performance in steady flow," *Proceedings of the Institution of Mechanical Engineers, Part C: Journal of Mechanical Engineering Science* **208**(4), pp. 253–266, 1994.

[6] M. Mao, W. Hu, Y.-T. Choi, N. M. Wereley, A. L. Browne, J. Ulicny, and N. Johnson, "Nonlinear modeling of magnetorheological energy absorbers under impact conditions," *Smart Materials and Structures* **22**(11), p. 115015, 2013.

[7] N. Rosenfeld and N. Wereley, "Volume-constrained optimization of magnetorheological and electrorheological valves and dampers," *Smart Material Structures* **13**, pp. 1303–1313, 2004.

[8] I. Grant and W. Phillips, *Electromagnetism*, Chichester, John Wiley and Sons, 2nd ed., 1990.



Downloaded From: https://www.spiedigitallibrary.org/conference-proceedings-of-spie on 25 Jul 2019
Terms of Use: https://www.spiedigitallibrary.org/terms-of-use